

Research on Resonance Coefficient of Building

Chuan Chen¹ & Xue Lingya¹

¹ Taizhou Vocational and Technical College, China

Correspondence: Xue Lingya, Taizhou Vocational and Technical College, Zhejiang, Taizhou, China. E-mail: 395419314@qq.com

Received: November 1, 2024; Accepted: December 29, 2024; Published: December 31, 2024

Abstract

In recent years, earthquakes have occurred frequently in the northwest region of China, causing casualties, house collapses, and serious economic losses. Therefore, a rough residential building with three floors was built in a remote area to understand the impact of resonance coefficient on houses and select the most suitable resonance coefficient for human habitation. The experimental tools include accelerators, data processors, vibration tables, buckets, laptops, etc. Creating different frequencies by rotating the vibration table at different speeds, normalize the values using an acceleration processor, select the relationship between frequency and acceleration, and draw a curve graph to select the resonant frequency.

Keywords: resonance frequency, acceleration, dynamics

1. Introduction

Resonance will bring great harm to the dynamic problems including the train moving on embankments and bridges. This chapter uses the shaker test to illustrate the importance of the resonance effect. Although the test object is a building, it still can be applied to the moving train problems. This chapter mainly introduces the natural frequency of the building and its magnification factor. We use the shaker load with different frequencies to rotate the one-story building, and record the acceleration at several locations. Then we can find the natural frequency of the building and its magnification factor.

2. Literature Review

2.1 Literature Review About the Effect Of Frozen Soil on Railway

Zhu et al. (2010) studied residual deformation laws and dynamic subsidence prediction model of permafrost subgrade under train traffic based on dynamic triaxial test at low temperature of the frozen clay from the Beiluhe permafrost subgrade along the Qinghai-Tibet Railway (QTR). Zhao et al. (2015) investigated dynamic characteristics of heavy-haul railway subgrade under vibratory loading in cold regions and tested low-temperature dynamic triaxial with multi-stage cyclic loading process. Zhang et al. (2015) studied the roadbed temperature distribution rules in seasonally frozen regions, and proposed an empirical model based on three years' field monitored temperature data. Zhang et al. (2016) presented the field data of frost heave and frost depth observed along the railway. And analyzed alternative mechanisms that have been considered to have caused the observed frost heave. Yue et al. (2015) tested subgrade sections of the Harbin-Qiqihar Line, a special line for passenger transport built in the deep seasonal frozen soil regions of China, to monitor field temperatures. Yu et al. (2013) monitored Ground temperature and settlement at different soil layers in four typical sections of the Qinghai-Tibet Highway (QTH) and tested one section of a newly built test (NBTR) in Beilu River basin. Wu et al. (2010) addressed those areas where no measures were taken and presented analysis of the variation of soil temperatures under the embankment in seasonal frozen soil areas, degrading permafrost areas, and warm and cold permafrost areas. Wu et al. (2002) reviewed the nature of frozen soil research along the Qinghai-Tibet Highway between 1993 and 2000. Wu et al. (2007) built an experimental railway section and collected the data within one freeze-thaw cycle in order to study the cooling mechanism of embankment with block stone interlayer under open and closed conditions. Wu et al. (2015) made the daily soil temperature measurements at 10 sites within five alpine ecosystems in the Beiluhe area of the central Qinghai-Tibet Plateau between 2002 and 2012.

2.2 Literature Review about the Foundation Settlement

Zhang and Hu. (2007) conducted a theoretical study on the determination of the allowable differential settlement. Yau. (2009) investigated the dynamic response of a maglev (magnetically levitated) vehicle traveling over a series of guideway girders undergoing ground support settlement. Xia. (2006) established a dynamic model of coupled

train-bridge system subjected to earthquakes based on the theory of dynamic wheel-rail interactions, in which the non-uniform characteristics of the seismic wave input from different foundations are considered. Paixao et al. (2015) studied the influence of settlement profiles on the train-track system. Mauer (1995) presented a dynamic settlement model and developed the simulation of track settlement behaviour under rail traffic. Kouroussis et al. (2016) aimed to identify the main components which influence the generation and the propagation mechanisms of railway-induced ground vibrations. Duhamel et al. (2008) presented a reduced scale experiment with three sleepers to study the dynamic behavior and the settlement of ballasted tracks. Dahlberg (2001) reviewed and commented upon mathematical models to simulate railroad track settlements.

3. Theoretical Framework

3.1 The Experiment Equipment

The accelerometer as shown in Figure 1 is one of the most important equipment in the experiment. It can measure acceleration in three directions: X, Y, Z. The sensitivities of the acceleration is 1V/98gal.

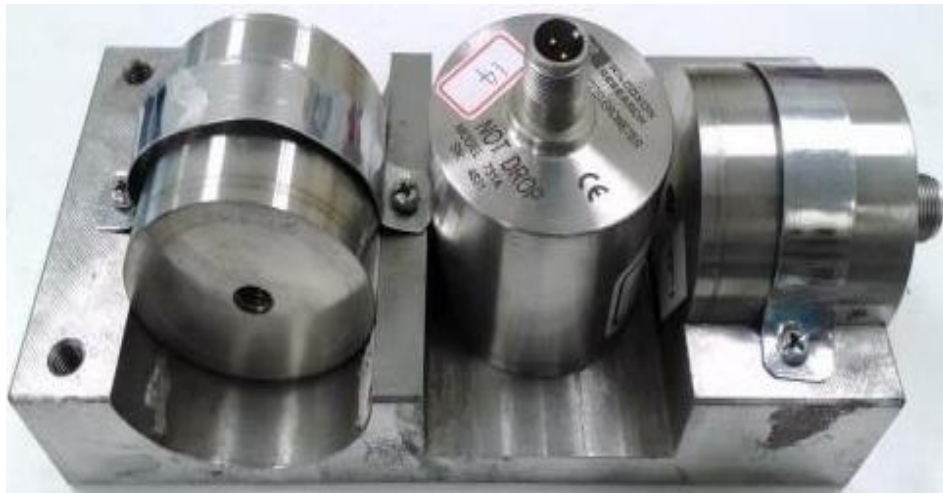


Figure 1. Accelerometers

The Integrator as shown in Figure 2 can supply the voltage to the accelerometer and convert the physical vibration to the voltage value. It can receive signals from the accelerometer. There are four channels in the integrator as shown in Figure 3,4. It can export four accelerations and four velocities.



Figure 2. Top view of the Integrator



Figure 3. Left side view of the house Integrator



Figure 4. Right side view of the house Integrator

Data capture device as shown in Figure 5 can send the data to the computer, There are 32 analog inputs, 2 analog outputs, 8 digital inputs, 8 digital outputs in the data capture device.

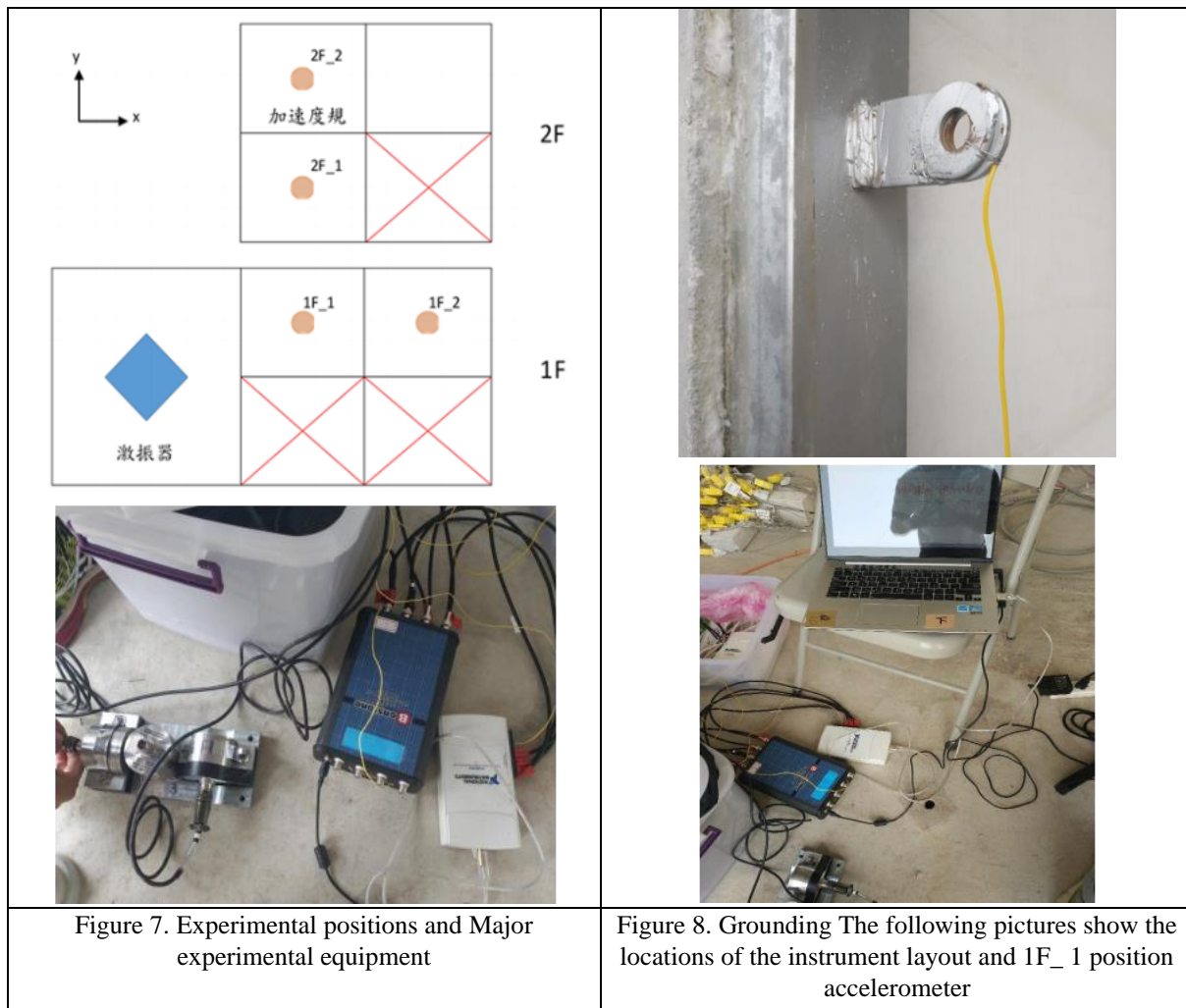


Figure 5. Data capture

The computer as shown in Figure 6 is used to display experimentally measured data and process data.



Figure 6. Computers



3.2 Experiment Procedure

The experiment can be divided into three parts, the first part is to set the instruments, the second part is to use the MK-155U eccentric mass vibrator system to shake the real size steel house, and finally the data from the

experiment is analyzed. In the first part, we setup four experimental instruments as shown in Figure 7~10. Each measuring instrument contains a set of accelerometers, an AD converter, an integrator and a computer. In order to eliminate the noise from the measurement, we ground the instrument to solve the noise problem as shown in Figure 8. In the second part, we used the Toshiba exciter (Fig 11) to control the MK-155U eccentric mass vibrator system to swing the structure. Finally, we use gf program to analysis the data.

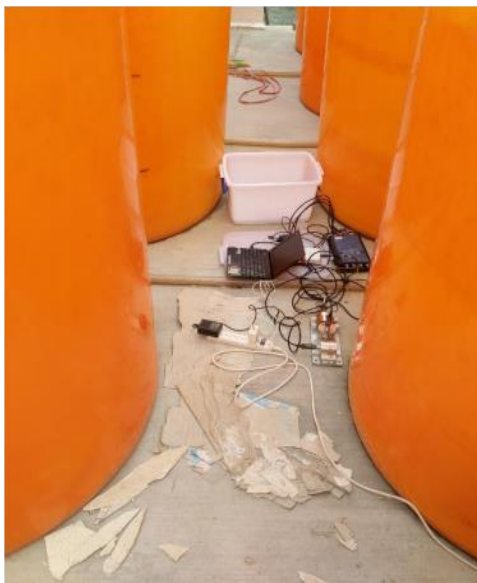


Figure 9. 1F_2 position accelerometer and 2F_1 position accelerometer



Figure10. 2F_2 position accelerometer



Figure 11. Toshiba drive

First, we give the Toshiba drive power. Then, turn the potentiometer until it points to the black point. Next, press the RUN button to operate the vibrator, and rotate the frequency controller to adjust the frequency. In this experiment, our frequency order is 4.0→4.1→4.2→4.3→4.4→4.5→4.6→4.7→4.8→4.9→5.0→5.1→5.2→5.3→5.4→5.5→5.6. The shaker will Rotate for 5 minutes at each frequency. After that, we use the frequency controller to adjust the frequency from 4.3 to 0 and press the STOP button to finish the experiment. Finally, turn down the potentiometer and turn off the power. We can get the measured data from the computer.

3.3 The Measurement Program (aa Program)

The experiment uses aa program to read the acceleration voltage of each station. The conversion relationship between voltage and acceleration is (10Volt=1g=980gal). We can get the data value of the acceleration through this conversion relation.

4. Analysis Date

4.1 1F_1 Data Measured by the Station

1F_1 is one of the acceleration stations which are erected on the ground floor of the building(Fig 2.6), Compared with 1F_2 station, The station is closer to the shaker system. 1F_1 station can be low-pass filtered by the gf program in X-direction acceleration. Removing the noise which is above 10Hz, and set up 1F_1 station X-direction acceleration time-lapse which is shown in Fig 12.

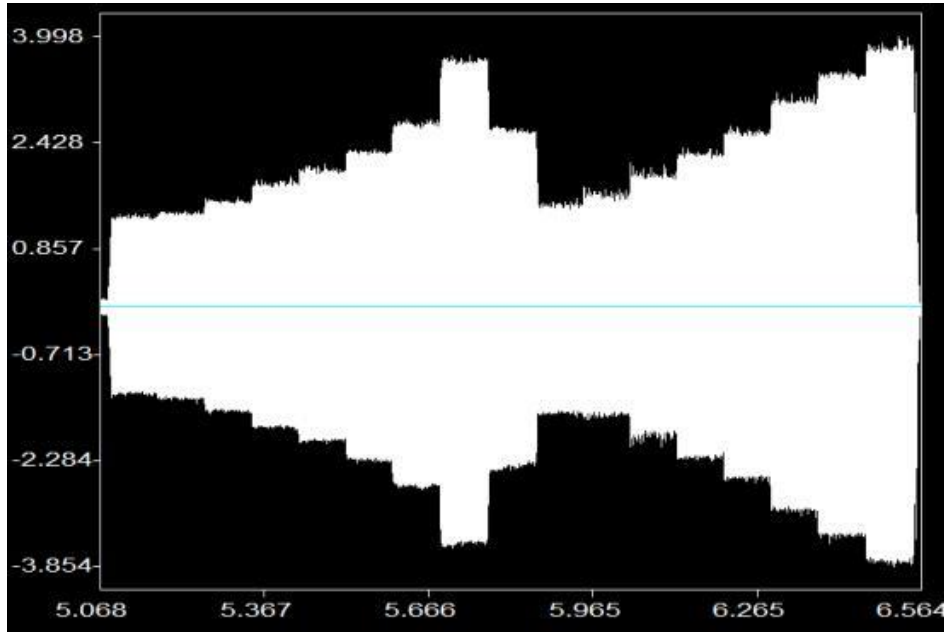


Figure 12. The first floor (1F_1) X-direction acceleration time diagram

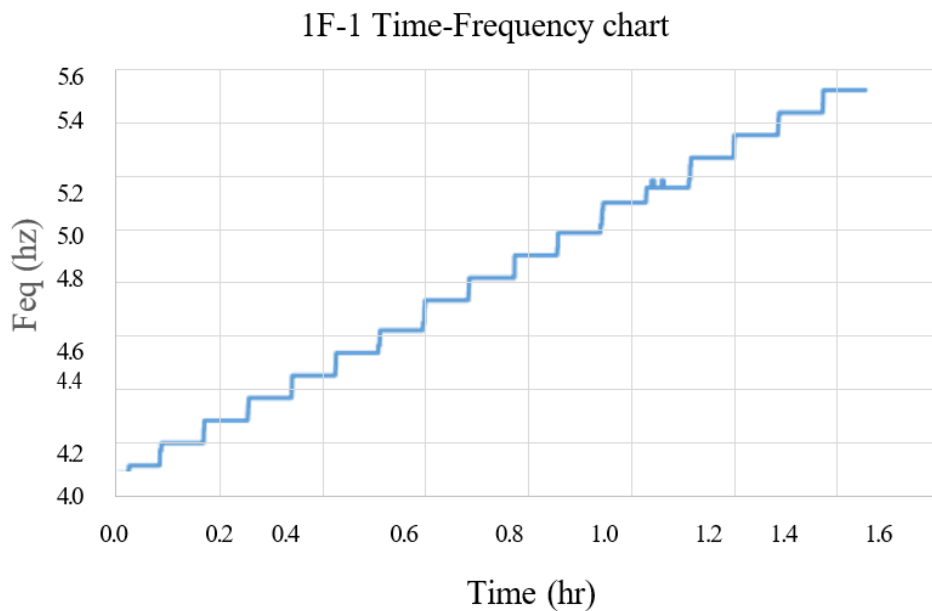


Figure 13. The first floor (1F_1) X-direction Frequency time diagram

Since the initial force of the shaker is proportional to the square of the frequency. We divide the spectrum amplitude of the FFT by the square of the frequency. We can get the FFT normalized amplitude as shown in Fig 14. The spectrum analysis shows the resonance of the building. It can be seen from the Fig 14 that the peak occurs at 4.7Hz. So, the resonance frequency in the X direction at 1F_1 station is 4.7Hz.

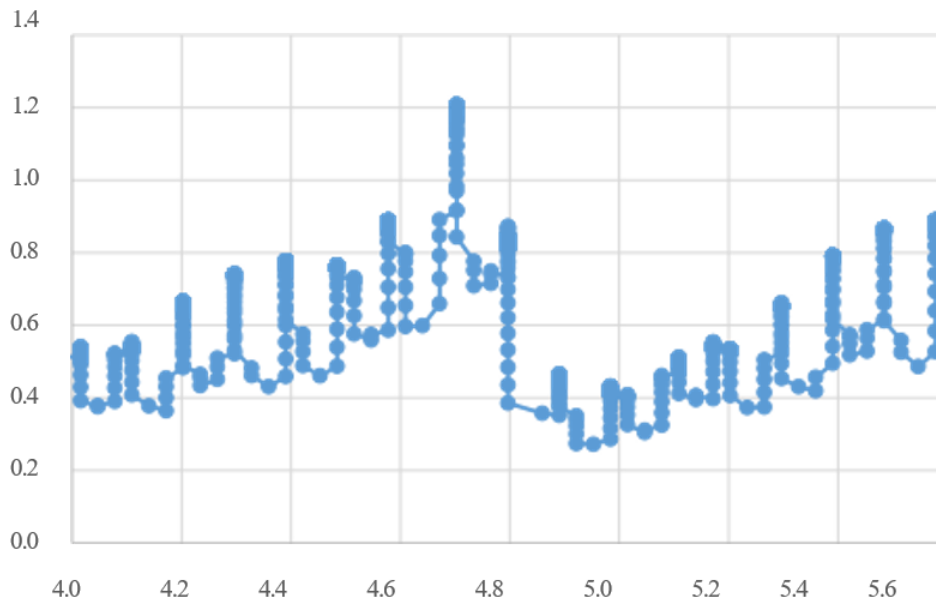


Figure 14. The first floor (1F_1) X-direction Spectrum

4.2 1F_2 Data Measured by the Station

Similarly, we can set up the 1F_2 station X-direction acceleration time-lapse which is shown in Fig 15 and get the frequency duration chart (Fig 16), FFT normalized amplitude (Fig 17).

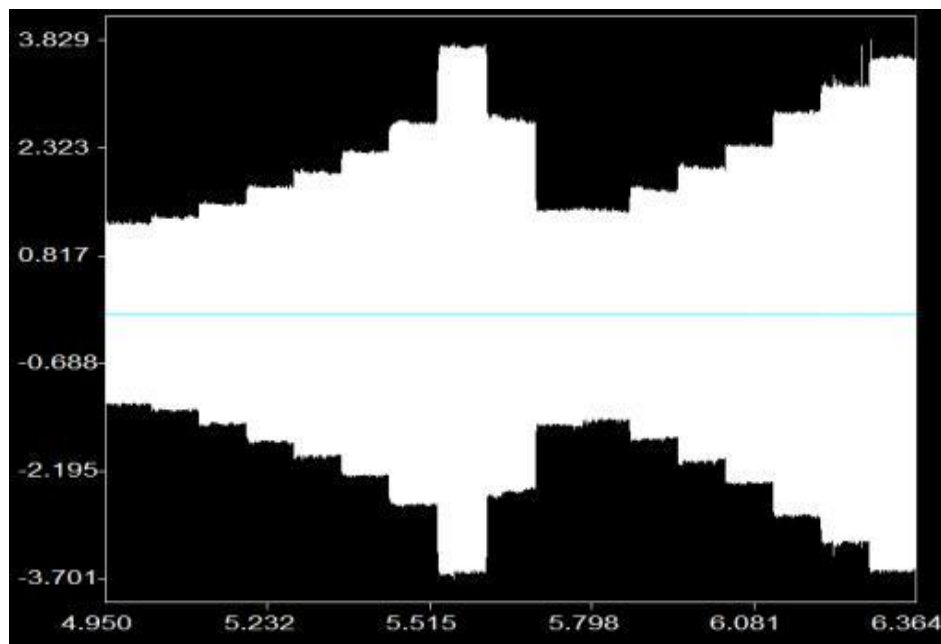


Figure 15. The first floor (1F_2) X-direction acceleration time diagram

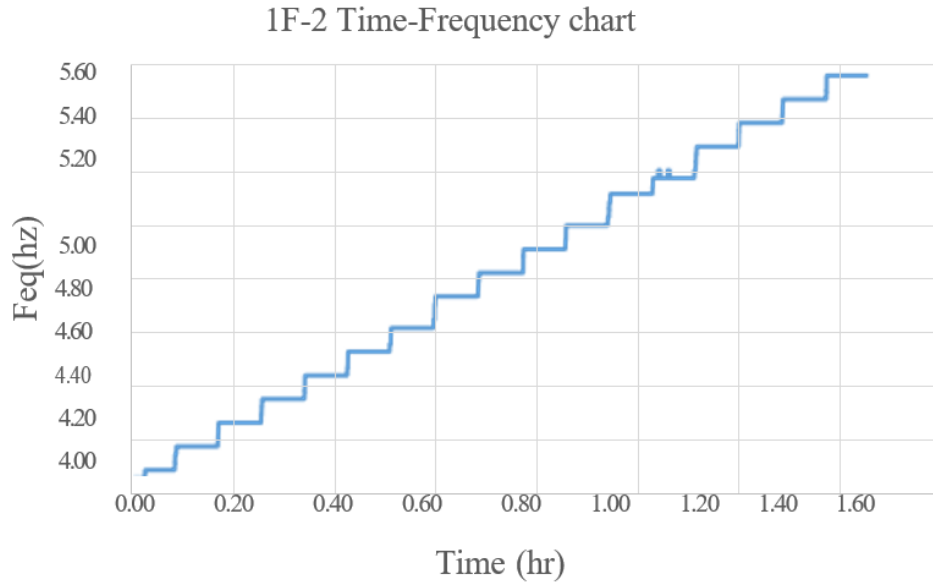


Figure 16. The first floor (1F_2) X-direction Frequency time diagram

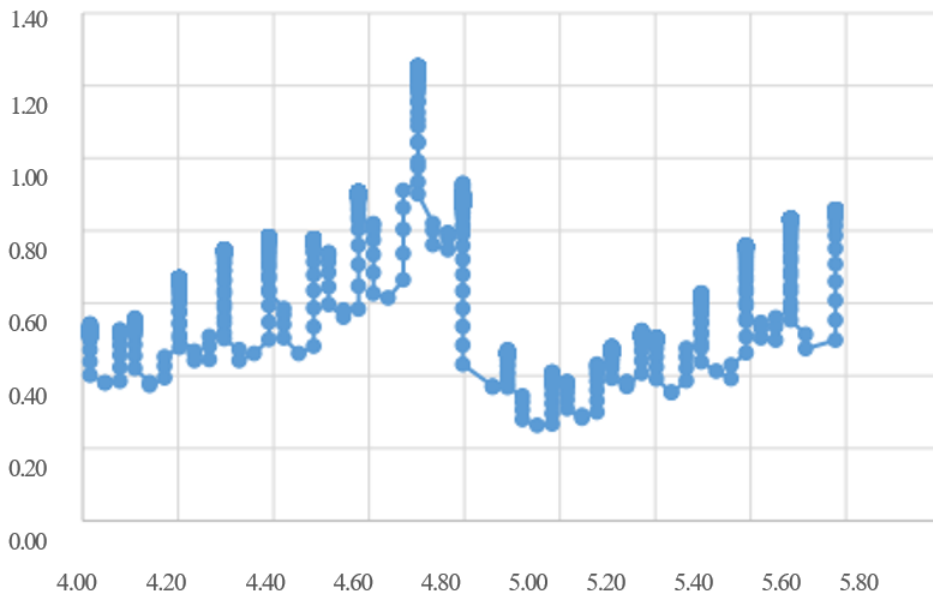


Figure 17. The first floor (1F_2) X-direction Spectrum

By comparing the differences between Fig 12 and Fig15 .We can find that the acceleration of the 1F_2 station is similar to 1F_ 1, but the first is a little smaller than that of the 1F_ 1 station. This is because the two stations are both located on the first floor. But the distance from station 2 to the shaker is a little longer than the distance from station 1 to the shaker. According to the two charts Fig 13 and Fig 16. We can easily find the results are the same, because the shaker gives the same frequency but has nothing to do with the distance. The resonance frequency can be found from the Fig 2.17. The peak occurs at 4.7Hz, so the resonant frequency is 4.7Hz which is as the same as the resonance frequency in X direction at 1F_ 1 station.

4.3 2F_1 Data Measured by the Station

2F_ 1 is one of the acceleration stations which are erected on the second floor of the building (Fig 7). 2F_ 1 station can be low-pass filtered by the gf program in X- direction acceleration. Removing the noise which is above 10Hz, and set up 2F_ 1 station X-direction acceleration time-lapse which is shown in Fig 18.

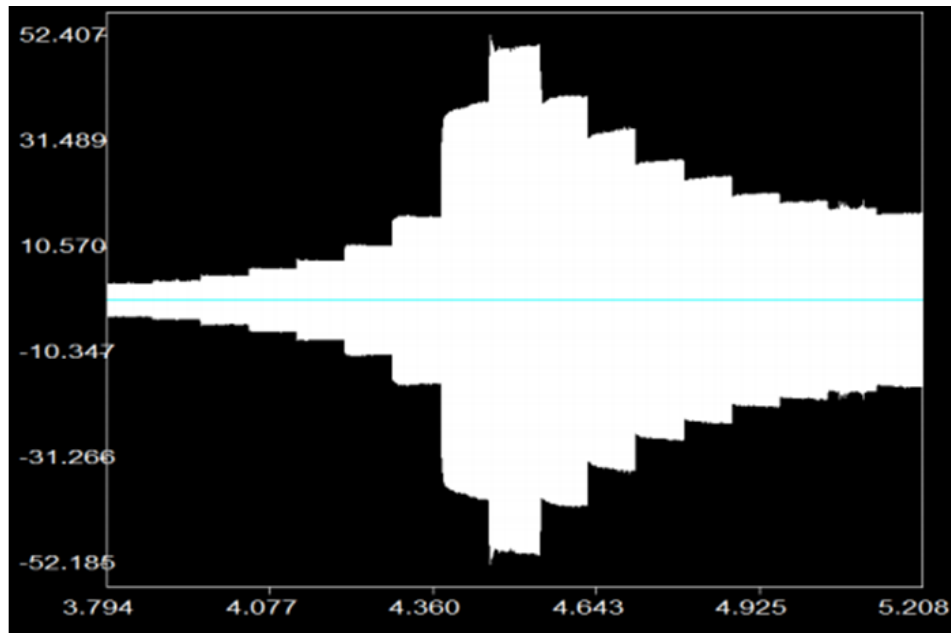


Figure 18. The second floor (2F_1) X-direction acceleration time diagram

Comparing with Fig 12. The acceleration numerical value can be found significantly larger than that on the first floor. Next, converting the acceleration time-lapse by FFT through the gf program. The sampling method is every 14 as agrid, and every 1 second FFT conversion. Then, we can get the frequency duration chart as shown in Fig 19.

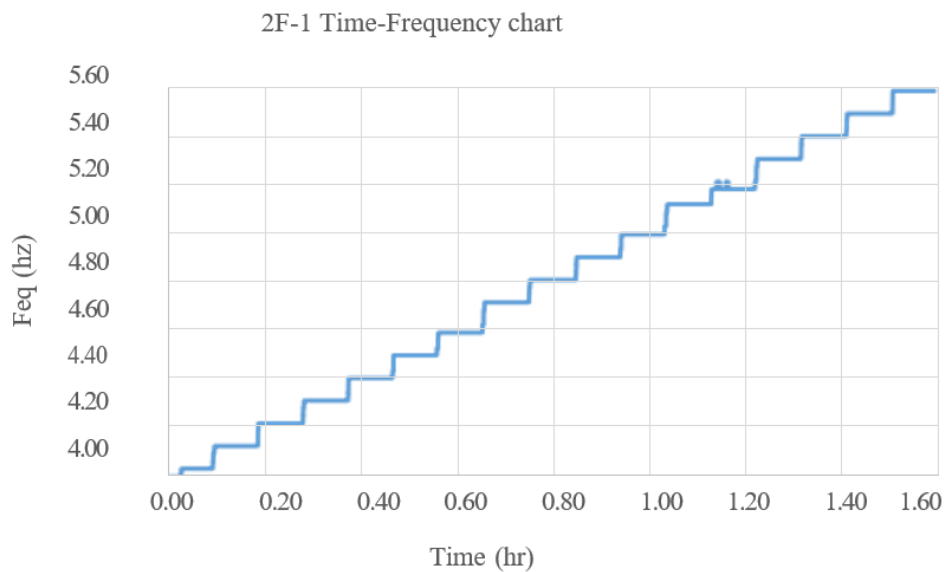


Figure 19. The second floor (2F_1) X-direction Frequency time diagram

Comparing with Fig 13. It can be found the results are the same, because the shaker gives the same frequency and has nothing to do with the floor height.

Since the initial force of the shaker is proportional to the square of the frequency. We divide the spectrum amplitude of the FFT by the square of the frequency. We can get the FFT normalized amplitude as shown in Fig 20.

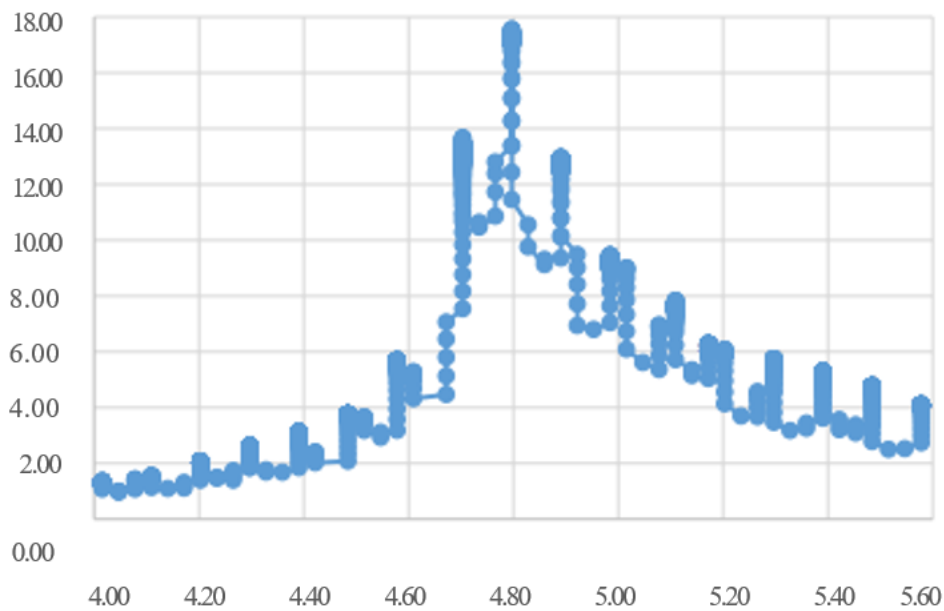


Figure 20. The second floor (2F_1) X-direction Spectrum

The spectrum analysis shows the resonance of the building. It can be seen from the Fig 20 that the peak occurs at 4.8Hz. So, the resonance frequency in the X direction at 2F_1 station is 4.8Hz. Compared with the FFT normalized amplitude of the first floor, we can find that the normalized amplitude of the second floor is about 13 times larger than that of the first floor when the frequency is 4.8Hz.

4.4 2F_2 Data Measured by the Station

Similarly, we can set up the 2F_2 station X-direction acceleration time-lapse which is shown in Fig 21, and get the frequency duration chart(Fig 22), FFT normalized amplitude(Fig 23).

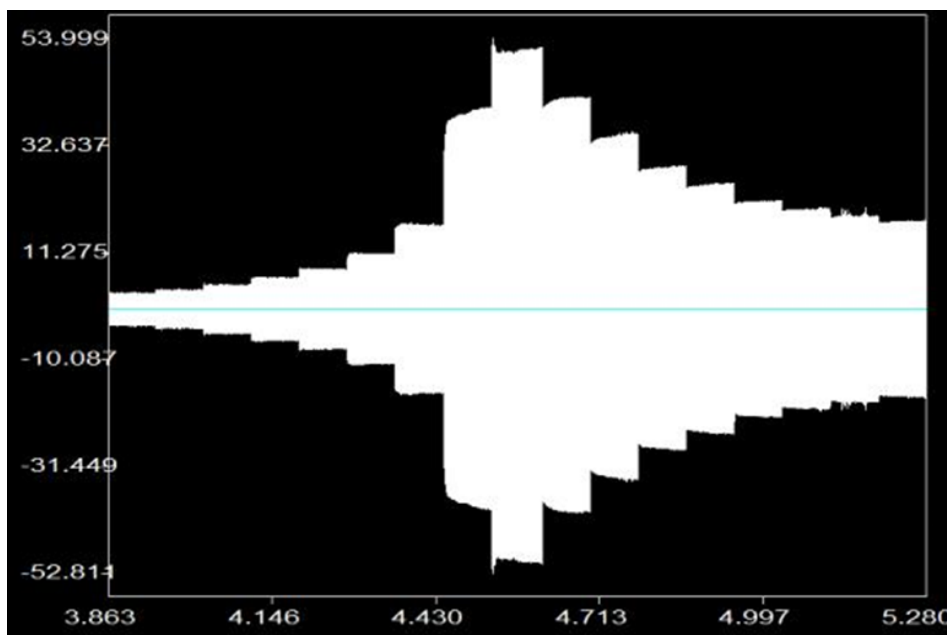


Figure 21. The second floor (2F_2) X-direction acceleration time diagram

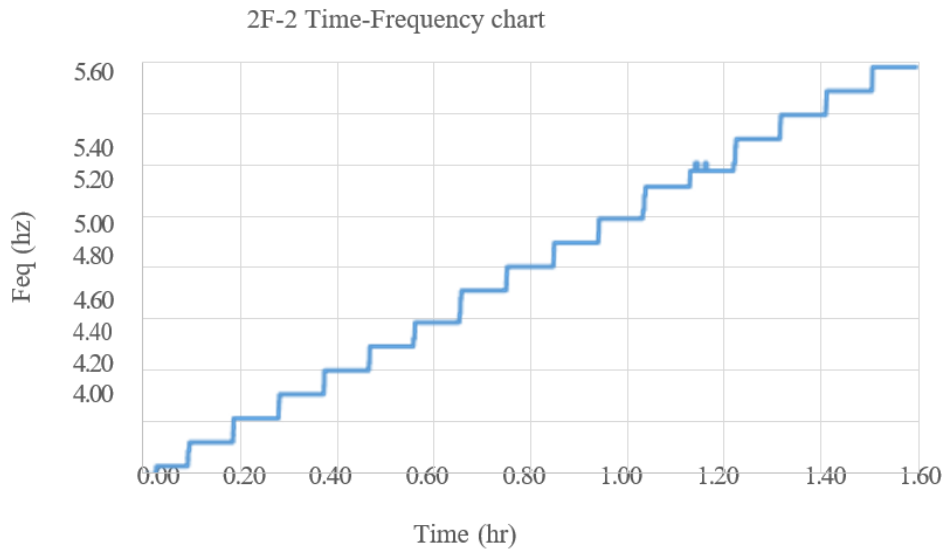


Figure 22. The second floor (2F_2) X-direction Frequency time diagram

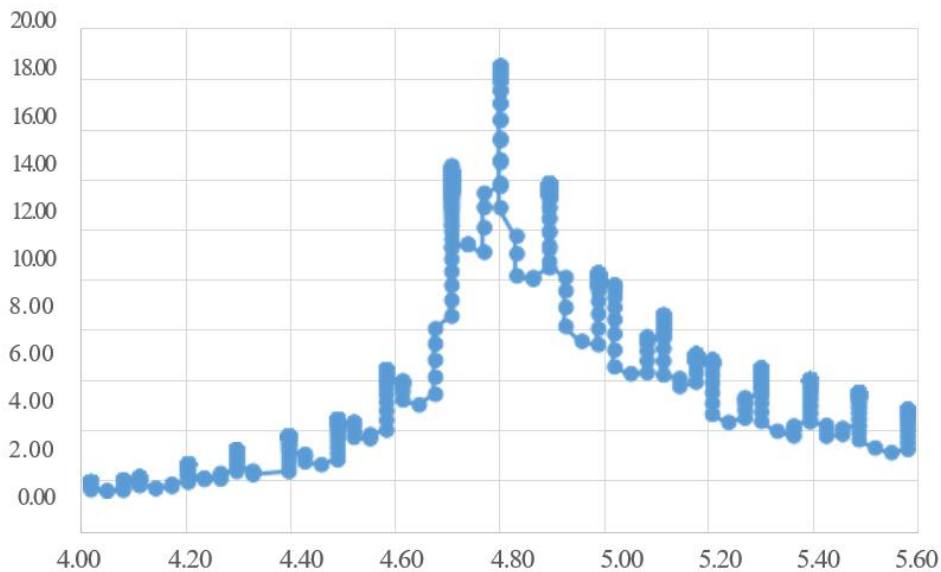


Figure 23. The second floor (2F_2) X-direction Spectrum

We can find that the maximum acceleration of the second floor is about 40gal from Fig 19 , which means it is far greater than the maximum acceleration on the first floor. According to the Fig 22 , Fig 13 and Fig 19. It can be found that the results are the same, which means the shaker gives the same frequency and has nothing to do with the floor height or distance. Fig 23 shows the resonance of the building. It can be seen from the Fig 23 that the peak occurs at 4.8Hz, so the resonance frequency in the X direction at 2F_2 station is 4.8Hz.

Finally, we plot the acceleration chart for each station at different external force frequencies (Table 1) and the acceleration frequency chart (Fig 24) and magnification factor frequency chart for each station (Fig 25).

Table 1. Acceleration chart of different stations at different Frequency

Frequency (Hz)	1F_1	1F_2	2F_1	2F_2
4.0	1.335	1.292	2.862	2.940
4.1	1.370	1.341	3.770	3.867
4.2	1.540	1.504	4.905	4.562
4.3	1.761	1.782	5.813	6.185
4.4	2.017	1.994	7.630	7.807
4.5	2.290	2.272	10.580	11.052
4.6	2.681	2.616	16.254	16.847
4.7	3.619	3.727	37.817	37.940
4.8	2.600	2.700	49.620	51.848
4.9	1.471	1.439	40.087	41.881
5.0	1.660	1.472	33.732	34.463
5.1	1.880	1.717	27.830	28.205
5.2	2.221	2.044	24.200	24.960
5.3	2.528	2.305	21.021	21.715
5.4	3.057	2.780	19.205	19.860
5.5	3.432	3.204	17.843	18.933
5.6	3.806	3.600	19.708	17.542

Acceleration -frequency chart of different stations

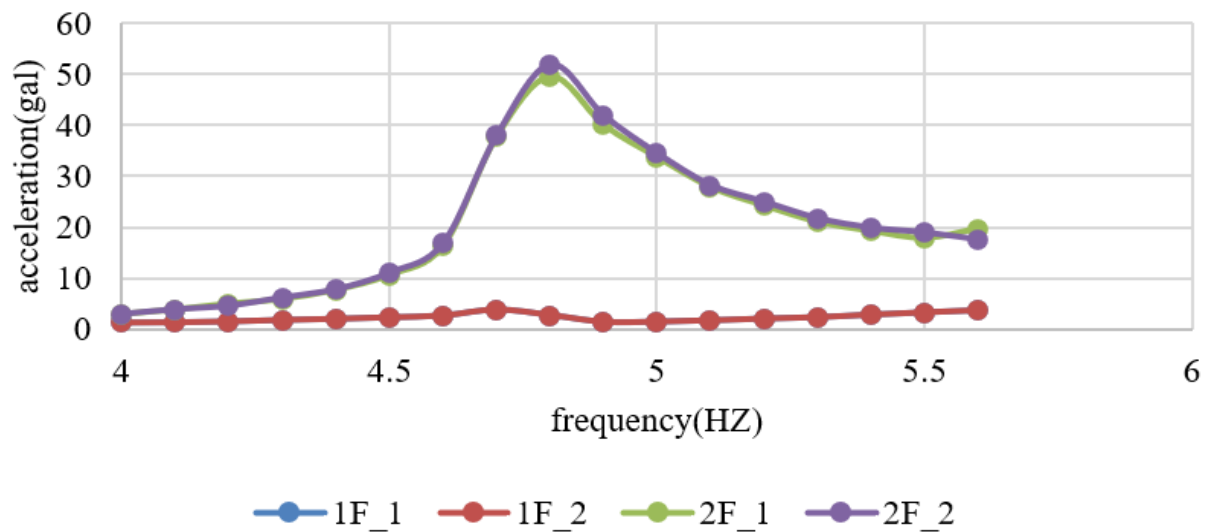


Figure 24. Acceleration frequency graph of each station

Magnification factor-Frequency

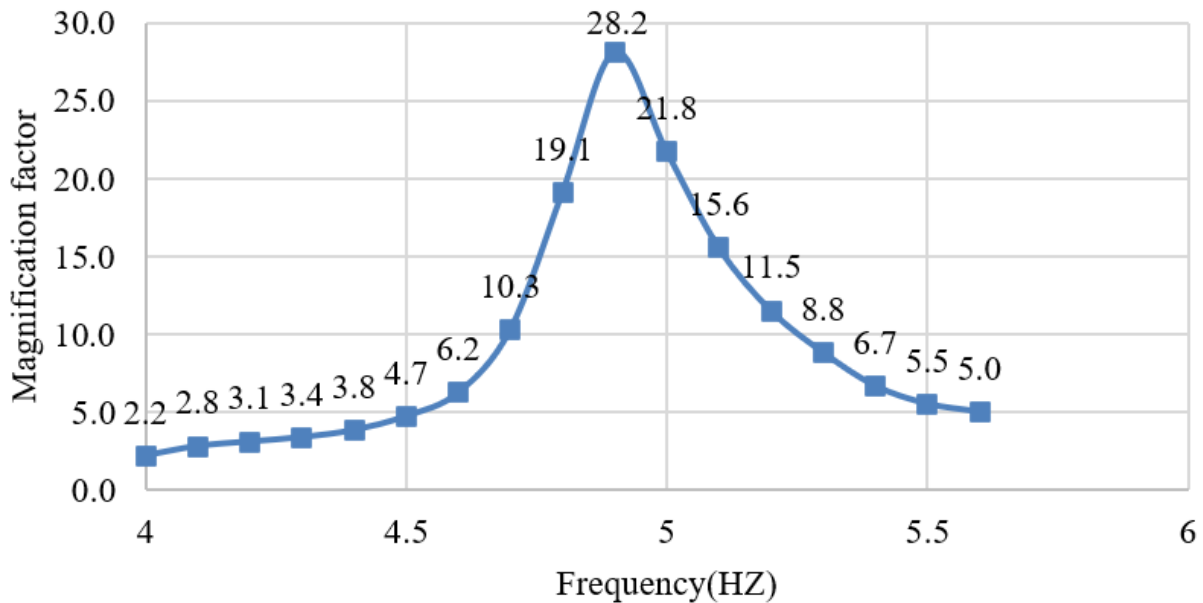


Figure 25. Magnification factor (2F / 1F) v.s. Frequency

5. Experimental Result

We found that the acceleration on the second floor is significantly larger than the acceleration on the first floor. The biggest difference occurs when the frequency is 4.9Hz. The calculation shows that the acceleration on the second floor is 28.2 times larger than that on the first floor.

6. Conclusion

The resonance causes a considerably large vibration of structures even though the source load is small, and this phenomenon has been validated in the shaker experiment of this thesis. Thus, the resonance should be avoided.

References

[1] Liu, P., Zhu, H., Yang, W., et al. (2020). Resonance and damping response of high-rise buildings caused by mechanical vibration. *Journal of Zhejiang University: Engineering Edition*, 54(1), 8. <https://doi.org/10.3785/j.issn.1008-973X.2020.01.012>

[2] Wang, J. (2020). Effect of damping and resonant frequency on the sound insulation performance of the floating floor slab. *Journal of Jiangsu Architecture Vocational and Technical College*, 20(3), 4.

[3] Huang, X. (2002). Research on low-frequency sound insulation factors affecting residential buildings. *Journal of South China University of Technology: Natural Science Edition*, 30(10), 4. <https://doi.org/10.3969/j.issn.1000-973X.2002.10.019>

[4] Feng, X. (2022). Study on the band gap characteristics of local resonant concrete slab (Doctoral dissertation). Inner Mongolia University of Science and Technology.

[5] Zhu, X. (2016). Vibration and acoustic radiation control of reinforced plates based on acoustic metamaterials (Doctoral dissertation). National Defense University of Science and Technology, Hunan.

[6] Fan, Y., Li, L., & Dang, R. (2013). Research on the weak signal detection method at an arbitrary large frequency based on stochastic resonance. *Journal of Instrumentation*, 34(3), 566–572. <https://doi.org/10.3969/j.issn.0254-3087.2013.03.013>

[7] Xia, J., Liu, Y., Ma, Z., et al. (2012). Study of weak signal detection based on modulation stochastic resonance. *Vibration and Impact*, 31(3), 5. <https://doi.org/10.3969/j.issn.1000-3835.2012.03.027>

[8] Zhao, W., Liu, J., & Yin, Y. (2011). Detection method and circuit design for medium and low frequency signals based on stochastic resonance principle. *Journal of Instrumentation*, 32(4), 8. <https://doi.org/10.3969/j.issn.0254-3087.2011.04.002>

- [9] Ran, C. (2024). Study on the dynamic response of house structure under blasting seismic wave (Doctoral dissertation). Wuhan University of Technology. <https://doi.org/10.3969/j.issn.1009-976X.2024.12.31>
- [10] Li, J. (2024). Analysis and study of the isolation effect of three-dimensional foundation isolation in houses (Doctoral dissertation). Xihua University.
- [11] Li, C. (2016). Research on the key problems of foundation design of large-scale seismic simulation vibration platform (Doctoral dissertation). Southeastern University. <https://doi.org/10.7666/d.Y3186352>
- [12] Lin, X. (2015). Environmental vibration and seismic safety analysis of slab high-rise residential buildings (Doctoral dissertation). Shanghai Jiao Tong University.
- [13] Yang, L., Zhou, X., Su, Y., et al. (2006). Variable stiffness protection device of foundation isolation building. *Journal of Beijing University of Technology*, 32(2), 7. <https://doi.org/10.3969/j.issn.0254-0037.2006.02.006>
- [14] Xu, G., Yao, L., Gao, Z., et al. (2008). Experimental study on large vibration table model of dynamic characteristics and dynamic response of side slope. *Journal of Rock Mechanics and Engineering*, 27(3), 9. <https://doi.org/10.3321/j.issn:1000-6915.2008.03.025>

Copyrights

Copyright for this article is retained by the author(s), with first publication rights granted to the journal.

This is an open-access article distributed under the terms and conditions of the Creative Commons Attribution license (<http://creativecommons.org/licenses/by/4.0/>).